

Smad1 signaling restricts hematopoietic potential after promoting hemangioblast commitment

Brandoch D. Cook,¹ Susanna Liu,¹ and Todd Evans¹

¹Department of Surgery, Weill Cornell Medical College, New York, NY

Bone morphogenetic protein (BMP) signaling regulates embryonic hematopoiesis via receptor-mediated activation of downstream SMAD proteins, including SMAD1. In previous work, we showed that *Smad1* expression is sufficient to enhance commitment of mesoderm to hemangioblast fate. We also found indirect evidence to support a subsequent repressive function for *Smad1* in hematopoiesis. To test this hypothesis directly, we developed a novel system allowing temporal control of *Smad1* levels by conditional knockdown in embryonic stem

cell derivatives. Depletion of *Smad1* in embryoid body cultures before hemangioblast commitment limits hematopoietic potential because of a block in mesoderm development. Conversely, when *Smad1* is depleted in FIK1⁺ mesoderm, at a stage after hemangioblast commitment, the pool of hematopoietic progenitors is expanded. This involves enhanced expression levels for genes specific to hematopoiesis, including *Gata1*, *Runx1* and *Eklf*, rather than factors required for earlier specification of the hemangioblast. The phenotype correlates with

increased nuclear SMAD2 activity, indicating molecular cross-regulation between the BMP and TGF- β signaling pathways. Consistent with this mechanism, hematopoiesis was enhanced when *Smad2* was directly expressed during this same developmental window. Therefore, this study reveals a temporally defined function for *Smad1* in restricting the expansion of early hematopoietic progenitors. (*Blood*. 2011; 117(24):6489-6497)

Introduction

Mammalian hematopoiesis begins on the yolk sac, generating a transient population of primitive erythrocytes, as well as a subset of definitive myeloid lineages.¹ Considerable progress has been made identifying the relevant signaling pathways that regulate early hematopoiesis.^{2,3} The bone morphogenetic protein (BMP) members of the TGF- β superfamily are particularly important in patterning the character of early embryonic tissue to generate ventral mesoderm,^{4,5} which serves as the origin of the developing hemangioblast, a cell type that is bipotent for the hematopoietic and vascular lineages.⁶ Forced expression of BMP ligands or signaling components expands hematopoiesis,⁷ while genetic deletion of *Bmp4* or its cognate receptor results in developmental arrest during gastrulation, with attendant failure to generate the mesodermal precursors from the epiblast that are required for hematopoietic development.^{4,8}

Key downstream effectors of TGF- β and BMP signaling are members of the SMAD family of transcription factors, that are activated by type I receptors through C-terminal serine/threonine phosphorylation, after ligand binding and subsequent trans-activation of type I/type II receptor heterodimers.⁹ There are 5 receptor-activated SMADs, or R-SMADS: SMAD2 and SMAD3 mediate the TGF- β /Activin/Nodal pathway, while SMADs 1, 5, and 8 respond to BMP signaling. *Smad1* and *Smad5* have roles in hematopoiesis, while *Smad8* is apparently not expressed in hematopoietic cells.¹⁰ Activated R-SMADs compete for access to a single coactivator or coSMAD, SMAD4, that when bound allows translocation of R-SMADs to the nucleus, where they bind and activate transcription of target genes within the context of multimeric

complexes.¹¹ The R-SMADs share a high degree of similarity in amino acid sequence, with SMAD1 and SMAD5 sharing approximately 92% identity in mouse; additionally, all of the relevant functional domains in R-SMADs are conserved, with DNA binding mediated via the N-terminal MH1 domain.

Regardless of the high degree of sequence similarity between SMAD1 and SMAD5, several studies revealed striking differences in their biology. Notably, while deletion of either gene results in early embryonic lethality, the underlying phenotypes are distinct. *Smad5*-null mice die around embryonic day 10 (E10) with gross defects in yolk sac vasculogenesis, and impairments in the developing gut and cardiac compartments.^{12,13} *Smad1*-null embryos, on the other hand, die at day E9.5 because of a failure in chorio-allantoic fusion.¹⁴ In addition, *Smad1* is required for development of extra-embryonic tissues and in regulation of visceral endoderm proliferation.¹⁵ In zebrafish, *smad5* and *smad1* are sequentially expressed during different stages of embryonic development, although they both function to impart ventralized character to mesoderm.¹⁶ Morpholino-based knockdown of *smad1* or *smad5* results in distinct and even opposite hematopoietic defects in zebrafish embryos, with *smad1* able to rescue the *smad5* morphant phenotype, but not vice versa.¹⁷

Embryonic hematopoiesis can be recapitulated faithfully in vitro using the embryonic stem cell/embryoid body (ES/EB) system, with the timing of progenitor commitment occurring similar to the mouse embryo.¹⁸ The early lethality caused by deletion of individual R-SMADs presents a challenge to understand their roles during specific stages of embryonic hematopoiesis.

Submitted October 7, 2010; accepted April 13, 2011. Prepublished online as *Blood* First Edition paper, April 22, 2011; DOI 10.1182/blood-2010-10-312389.

The online version of this article contains a data supplement.

The publication costs of this article were defrayed in part by page charge payment. Therefore, and solely to indicate this fact, this article is hereby marked "advertisement" in accordance with 18 USC section 1734.

© 2011 by The American Society of Hematology

Given evidence for their importance, and the regulatory potential for individual SMAD factors, we exploited the advantage of manipulating SMAD expression in the ES/EB system. We showed previously that *Smad1* expression is enriched in the BRY⁺/FLK⁺ subpopulation of blast colony-forming cells (BL-CFCs) that arises around day 3.5 of EB differentiation, and that has been identified as the in vitro equivalent of the hemangioblast.^{6,19} Furthermore, we used a conditional transgene expression system to show that a timed pulse of SMAD1 early in EB differentiation is sufficient to increase hematopoietic progenitors through expansion of the BL-CFC subset. Surprisingly, increased numbers of progenitors were not seen with continuous induction of *Smad1* transgene expression. In other words, *Smad1* expression needed to be transient to reveal the phenotype, suggesting that *Smad1* has both an early positive role, and then a subsequent inhibitory role in the proliferation, survival, or differentiation of hematopoietic progenitors.¹⁹

To test this hypothesis directly, we created a novel transgenic system allowing conditional shRNA-mediated gene-specific knockdown to explore the contribution of *Smad1* signaling to hematopoietic differentiation throughout embryoid body development. Our results demonstrate a repressive role for *Smad1* in regulating hematopoietic progenitor numbers, as we had previously hypothesized. In addition, our results suggest a mechanism involving competition for limited coSMAD that reveals cross-talk of the BMP and TGF- β signaling pathways.

Methods

Generation of inducible *Smad1* knockdown ES-cell lines

Three individual short interfering (22 nt) RNA target sites were identified in the mouse *Smad1* MH1 domain (NM_008539) using the Cold Spring Harbor Laboratory shRNA design protocol (<http://katahdin.mssm.edu/siRNA/RNAi.cgi?type=shRNA>). Complete hairpin oligonucleotides were designed with 5' and 3' miR-30 flanking sequence sufficient to allow intracellular RNA-induced silencing complex (RISC) processing, and used to PCR-amplify target sites with 5' *Xho1* and 3' *EcoRI* adapters as 130-bp fragments.²⁰ Individual shRNA hairpins were combined in tandem using restriction site adapters to subclone cassettes into the plox-IRES-EGFP vector. The resulting 3-hairpin construct (PIE-mi*Smad1*, 20 μ g) was cotransfected by electroporation with 20 μ g of pSALK-Cre into the parental ES-cell line AinV18 (8×10^6 cells). Multiple individual cell clones were isolated and expanded after selection with 300 μ g/mL G-418, and then tested for site-specific integration by PCR analysis of cDNA. Loxin primers: F5'-CTAGATCTCGAAGGATCTGGAG, R5'-ATACTTCTCGGCAGGAGCA. *Smad1* shRNA 22-mer sequences: a (GGUGAAGAAACUGAAGAAGAAG), b (AGCCGAGUAACUGCGU-CACCAU), and c (AAGGGACUACCUCUAUGUCAUUU).

ES-cell growth and differentiation

ES cells were maintained on irradiated mouse embryonic fibroblast (MEF) feeder cells in DMEM supplemented with 20% heat-inactivated ES-qualified FCS (Hyclone), 50 IU of penicillin (Cellgro), 50 μ g/mL streptomycin (Cellgro), Leukemia Inhibitory Factor (LIF; 2% conditioned medium), and 1.5×10^{-4} M monothioglycerol (MTG; Sigma-Aldrich). After serial depletion of mouse embryonic fibroblast (MEF) feeders, ES cells were allowed to differentiate as EBs in ethylene oxide-treated Petri grade dishes or in Aggrewell 400 plates (StemCell Technologies). EBs were cultured in IMDM supplemented with 15% FCS, 5% protein-free hybridoma medium (PFHM-II; Gibco), 2 mM L-glutamine (Cellgro), 0.5mM ascorbic acid (Cellgro), 200 μ g/mL transferrin (Roche), and 4.5×10^{-4} M MTG. For EBs harvested between days 3 and 4.5 of development, ES cells were plated at a density of 4×10^4 cells/mL culture medium, and for EBs harvested between days 5 and 6, ES cells were plated at a density of 8×10^3 cells/mL. Continuous *Smad1* knockdown via activation of

integrated shRNA hairpins was induced by addition of 1 μ g/mL doxycycline directly to either the ES-cell or EB-culture medium.

Colony assays

Differentiation of EB-derived cells into hematopoietic progenitor colonies was performed as described.^{19,21} Embryoid bodies contain subpopulations of cells that are asynchronously primed to undergo commitment to different early hematopoietic lineages. Therefore, primitive erythroid progenitors emerge from day 4 to day 7, with a peak around day 6 of differentiation. Similarly, there is an analogous distribution for in vitro definitive colony potential later in EB differentiation, overlapping with primitive erythroid potential. The time we probe, around day 6 is sufficient to interrogate both the primitive and initial definitive programs. Briefly, EBs were disaggregated by trypsinization, and single-cell suspensions were replated at a density of 1×10^5 cells/mL in IMDM containing 1% methylcellulose, 10% plasma-derived serum (PDS; Antech), 5% PFHM-II, 2mM L-glutamine, 0.25mM ascorbic acid, and 1.5×10^{-4} M MTG, supplemented with the following progenitor-specific cytokines: primitive erythroblasts (erythropoietin [EPO, 2 U/mL]); blast colonies (VEGF [5 ng/mL], SCF [5 ng/mL], IL-6 [10 ng/mL], 25% D4T endothelial cell-conditioned media); macrophages (IL-3 [1% conditioned media], M-CSF [5 ng/mL]); megakaryocytes (IL-3 [1% conditioned media], IL-11 [5 ng/mL], thrombopoietin [TPO, 5 ng/mL]); mixed colonies (SCF [5 ng/mL], IL-3 [1% conditioned media], G-CSF [30 ng/mL], GM-CSF [10 ng/mL], IL-11 [5 ng/mL], IL-6 [5 ng/mL], TPO [5 ng/mL], M-CSF [5 ng/mL]); and definitive erythrocytes (EPO [2 U/mL], TPO [5 ng/mL], SCF [5 ng/mL]). Colonies were counted under a light microscope at 10 \times magnification 4 days (EryP), 7 days (MacP, MegaP, EryD), or 9 days (Mixed) after plating. IL-3 was derived from media conditioned by CHO cells transfected with an IL-3 expression vector. EPO was obtained from the Mount Sinai Medical Center hospital pharmacy. All other cytokines were purchased from R&D Systems.

Quantitative RT-PCR

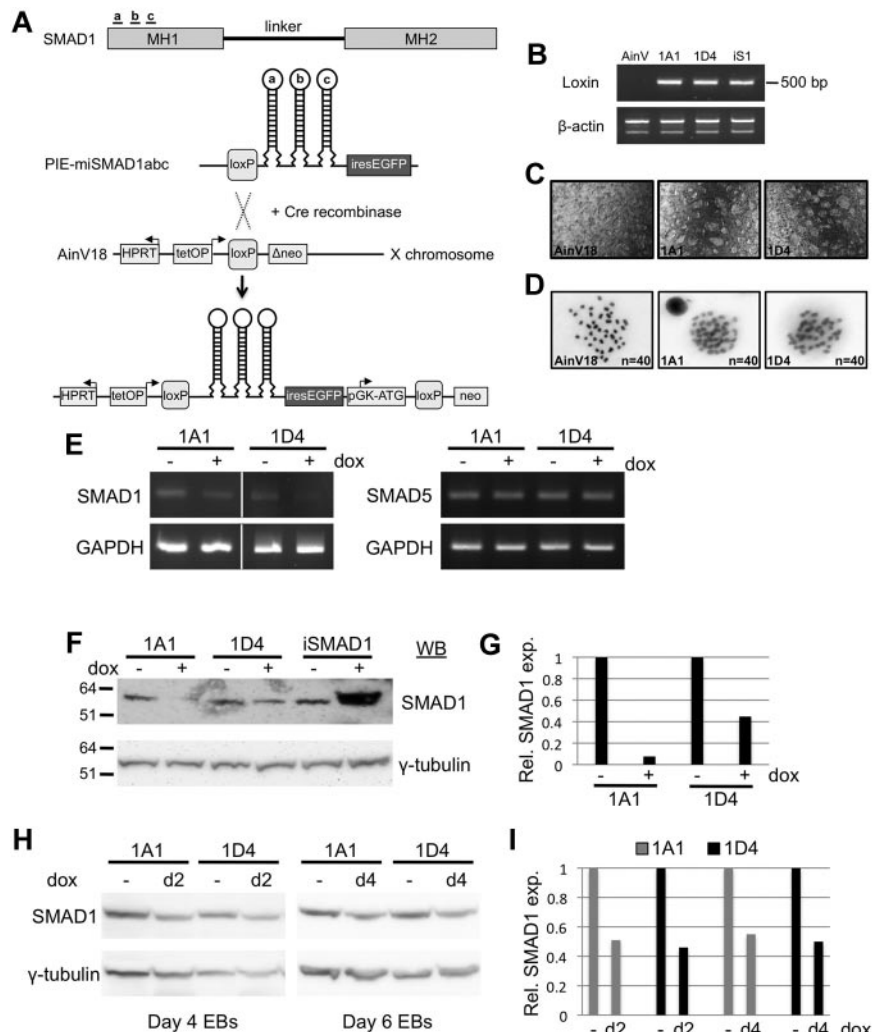
Smad1 knockdown was induced on day 2 or day 4 of EB development by addition of 1 μ g/mL doxycycline. Induced and control EBs were harvested at equivalent time points, and subjected to isolation of total RNA with TRIzol reagent (Invitrogen). One microgram of RNA was used in reverse transcription reactions using Superscript III First-Strand Synthesis kit (Invitrogen) to generate cDNA, which was analyzed directly by standard PCR, or diluted 1:40 in RNase-free H₂O for quantitative PCR (qPCR) with Sybr green using the Roche 480 II LightCycler and the $2^{-\Delta\Delta CT}$ method.²² PCR primers and qPCR primers are listed in the supplemental Table 1 (available on the *Blood* Web site; see the Supplemental Materials link at the top of the online article).

Western blotting

Whole-cell extracts were collected from ES or EB cultures in complete lysis buffer (20mM Tris, 150mM NaCl, 50mM NaF, 1% NP-40 substitute, 1% aprotinin, 1mM PMSF, 1mM Na₂VO₄). For cell fractionation experiments, EBs were collected, washed with ice-cold PBS and prepared essentially as described.²³ Coimmunoprecipitation was carried out using whole-cell lysates precleared with rabbit IgG (Jackson ImmunoResearch Laboratories) and protein A + G agarose beads (Santa Cruz Biotechnology), incubated overnight with anti-SMAD2 XP Ab (Cell Signaling) in a 1:50 dilution. Proteins were resolved by electrophoresis on pre-cast 10% NuPage Bis-Tris gels and transferred to nitrocellulose membranes using the iBlot system (both from Invitrogen). Membranes were blocked in 5% BSA in TBS + 0.5% Tween-20 and probed overnight with the following Abs: rabbit anti-SMAD1, anti-SMAD2/3, or anti-SMAD4 (Cell Signaling 9743, 3102, and 9515, respectively), mouse anti-SMAD5 (Invitrogen 39-5700), or mouse anti- γ -tubulin (Sigma-Aldrich). Loading of nuclear and cytoplasmic protein fractions was visualized by probing with Abs for histone deacetylase-1 (Cell Signaling 2062, rabbit Ab) and β -actin (Sigma-Aldrich, mouse mAb). Proteins were visualized with HRP-tagged secondary Abs (Bio-Rad or GE Healthcare) and West Pico chemiluminescence reagent (Pierce). Images were obtained and analyzed by densitometry to measure relative protein levels on a UVP Biospectrum 500 Imaging System.

Figure 1. Generation of inducible ES cells allowing temporal control of *Smad1* depletion.

(A) mi*Smad1abc*-IRES-EGFP ES cells were generated by combining the transgenic technique reported by Kyba et al (2002)²⁴ with the miR-30-based shRNA technique reported by Sun et al (2006).²⁰ Three unique shRNA target sites were identified in the MH1 domain of *Smad1*, and hairpins were designed containing the miR-30 flanking sequence required for endogenous RISC processing. Cre/loxP-mediated recombination of a construct containing hairpins a, b, and c in tandem results in site-specific integration into a position downstream of the HPRT locus on the X chromosome, and confers neomycin resistance, allowing selection and isolation of transgenic cell clones amenable to tet-on induction of *Smad1* knockdown, concomitant with GFP expression. (B) Genomic PCR analysis confirms single-copy site-specific integration of the shRNA-IRES-EGFP cassette. Two separate transgenic ES clonal cell lines are shown, 1A1 and 1D4. The parental AinV18 line serves as a negative control, and a transgenic iSmad1 clone that allows induced *Smad1* expression¹⁶ provides a positive control. (C) GFP expression is seen in 1A1 and 1D4 ES cells 24 hours after induction of mi*Smad1abc* hairpin expression, with parental AinV18 cells serving as negative control. (D) Analysis of metaphase karyotypes in the ES-cell lines, showing grossly normal chromosomal integrity in both clones, indistinguishable from parental AinV18 cells. (E) Representative RT-PCR analysis of *Smad1* transcript levels in 2 clonal lines 30 hours after induction, showing a decrease in *Smad1* transcript levels after addition of doxycycline, in contrast to unchanged levels of *Smad5* transcripts, with *Gapdh* as a loading control. (F) Analysis of SMAD1 protein levels 30 hours after induction in 2 separate transgenic clonal lines by Western blotting. Overexpression of iSmad1 using iSmad1 ES cells is used as a control to verify SMAD1 signal. (G) Densitometric analysis of SMAD1 protein levels normalized to the γ -tubulin loading control, demonstrating in a representative experiment the extensive knockdown (~60%-90%) in both cell lines. (H) Representative Western blotting analysis of SMAD1 protein levels 48 hours after induction in embryoid bodies using 2 independent clonal cell lines (I) Densitometric quantification of *Smad1* protein levels in a representative experiment, normalized to γ -tubulin controls, demonstrating approximately equivalent knockdown in 1A1 and 1D4 cell clones, with induction at either day 2 or day 4.



Flow cytometry

Control untreated and doxycycline-induced EBs were collected between days 3 and 6 of growth in differentiation medium by low-speed centrifugation, washed in PBS, and disaggregated by trypsinization. Cells were resuspended in ice-cold FACS buffer (PBS + 1% FCS + 1mM EDTA), and incubated with Abs for the relevant cell-surface proteins in V-bottom plates on ice. Cells (2×10^5) were stained with the following fluorophore-conjugated Abs and reagents: anti-c-KIT-APC (eBioscience 17-1171-83), anti-DPP4-APC (R&D Systems FAB9541A), anti-epCAM-PE (eBioscience 12-5791-81), or anti-FLK1-PE (BD PharMingen 555308). Controls included unstained and single Ab-stained samples. Individual live cells were gated by forward and side scatter, and 10 000 events were recorded and analyzed per sample using an Accuri C6 flow cytometer and De Novo FCS Express version 4 software. For some experiments, disaggregated day 4 EBs were stained in complete EB medium + 2mM EDTA with a 1:100 dilution of anti-FLK1-PE, sorted using a FACS Vantage SE (BD Biosciences), and recultured in a 1:1 ratio with cells derived from disaggregated day 2 AinV18 EBs with or without doxycycline, and subsequently analyzed by colony assays.

Results

Generation of a novel ES-cell line with the capacity for conditional depletion of *Smad1*

A system based on AinV murine ES cells has been described by Daley, Kyba, and colleagues for inducible control of transgene

expression.^{19,24} The AinV parental cell line has the coding sequences for the reverse tet-transactivator (rtTA) pre-targeted at the constitutively active Rosa26 locus, the rtTA operator site inserted near the HPRT locus, and just downstream of the operator site is a loxP site and a defective neomycin phosphotransferase gene. We adapted this system for the conditional expression of tandem shRNA hairpin modules specific for Smad1. The modules contain flanking 5' and 3' sequence from the mouse miR-30 gene that promote processing of hairpins by the intrinsic cellular RNA interference apparatus to generate functional siRNA molecules.²⁰ Three separate hairpins were designed to target the *Smad1* MH1 domain and cloned in tandem into the plox-IRES-EGFP vector using restriction site adapters, as shown in Figure 1A. The complete 3-hairpin construct, mi*Smad1abc*-IRES-EGFP, was coelectroporated with a vector expressing Cre recombinase into the parental AinV18 ES-cell line. Cre/loxP-mediated homologous recombination was selected using G418 by restoration of the neoR gene, and resulted in a single, site-specific insertion of the tet-inducible shRNA cassette into the X chromosome with IRES-driven EGFP as a reporter (Figure 1A).

We isolated multiple G418-resistant ES-cell clones (miSmad1ES), and examined them for site-specific integration of *Smad1* shRNAs (Figure 1B) and doxycycline-induced GFP expression (Figure 1C). Next, we evaluated genome integrity using chromosome spreads to assess ploidy in the cell lines. In both

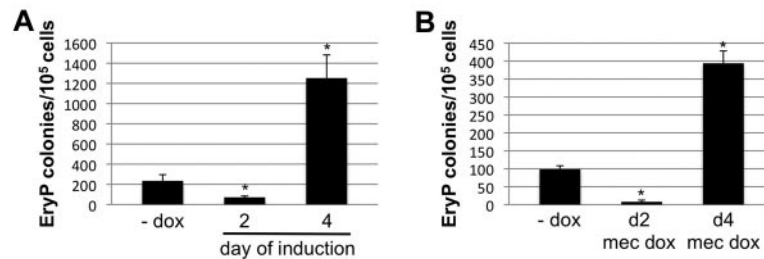


Figure 2. Early or late depletion of *Smad1* has opposite effects on primitive erythroid potential. (A) The primitive EryP colony-forming potential was analyzed for EBs derived from a representative mi*Smad1* ES-cell clone. *Smad1* knockdown was induced by 1 μ M doxycycline treatment starting either 2 or 4 days after initiation of growth in EB culture medium permissive for differentiation. The EBs were harvested at day 5.75 and recultured in 2 U/mL EPO in semisolid methylcellulose medium. Erythroid colonies were counted 4 days later, and the EryP potential of induced cells was compared with untreated cells. Results are shown as total mean colony number counted in each experimental condition, and each graph is a representative result from a pool of at least 4 independent experiments, each done in triplicate. (B) The EryP colony assays were repeated with the addition of doxycycline to the methylcellulose, to rule out potential confounding effects of doxycycline on cell differentiation.

mi*Smad1* lines tested, chromosome number did not deviate from the expected 40, and karyotypes were indistinguishable on a gross morphologic level compared with the AinV18 parental cells (Figure 1D). Data from 2 representative independent clones, 1A1 and 1D4, are shown in Figure 1 for purposes of ES-cell line validation. All following experiments were performed using both lines, which were found to be phenotypically similar, although only data for clone 1D4 is shown in subsequent figures. At 30 hours after addition of 1 μ M doxycycline to mi*Smad1* ES-cell cultures, *Smad1* RNA levels were clearly reduced according to semiquantitative RT-PCR analysis, while *Smad5* transcript levels remained constant (Figure 1E). Likewise, 30 hours after shRNA induction, SMAD1 protein levels were decreased in both ES-cell clones, determined by Western blotting experiments (Figure 1F). As a control, the previous line we had generated for induced expression of *Smad1* (i*Smad1*ES¹⁹) was included in this analysis, further validating that the depletion using the mi*Smad1* lines was because of shRNA expression rather than an indirect effect of doxycycline or some other component in the system. The graph in Figure 1G shows densitometric analysis of a representative experiment, with *Smad1* expression normalized to the γ -tubulin loading control, documenting an approximately 90% depletion of *Smad1* protein in clone 1A1 and 60% in clone 1D4. In multiple independent experiments mi*Smad1* lines were depleted of SMAD1 on induction within this typical range. Induction at day 2 or day 4 during EB differentiation resulted in approximately equivalent SMAD1 knockdown in cell clones 1A1 and 1D4 (Figure 1H and 1I). Therefore, while the lines do not eliminate SMAD1, induction of shRNAs reliably depleted SMAD1.

Inducible knockdown of *Smad1* before or after the hemangioblast stage of EB development has opposite effects on primitive erythroid progenitors

To study the contribution of *Smad1* signaling to embryonic hematopoiesis, we used conditional depletion of *Smad1* in the embryoid body system. Differentiating EBs recapitulate germ layer commitment in vitro, and disaggregation of EBs followed by reseeding in semisolid media with the relevant cytokines facilitates a quantitative assessment for progenitor numbers associated with primitive and early definitive hematopoiesis.²⁵ We showed previously that forced expression of *Smad1* during a limited developmental window around day 2, before hemangioblast formation, expands the progenitor population committed to hemato-vascular development.¹⁹ In contrast, when *Smad1* knockdown was induced using the mi*Smad1* lines beginning at day 2 of EB differentiation, there was a major reduction in primitive erythroid (EryP) colony formation

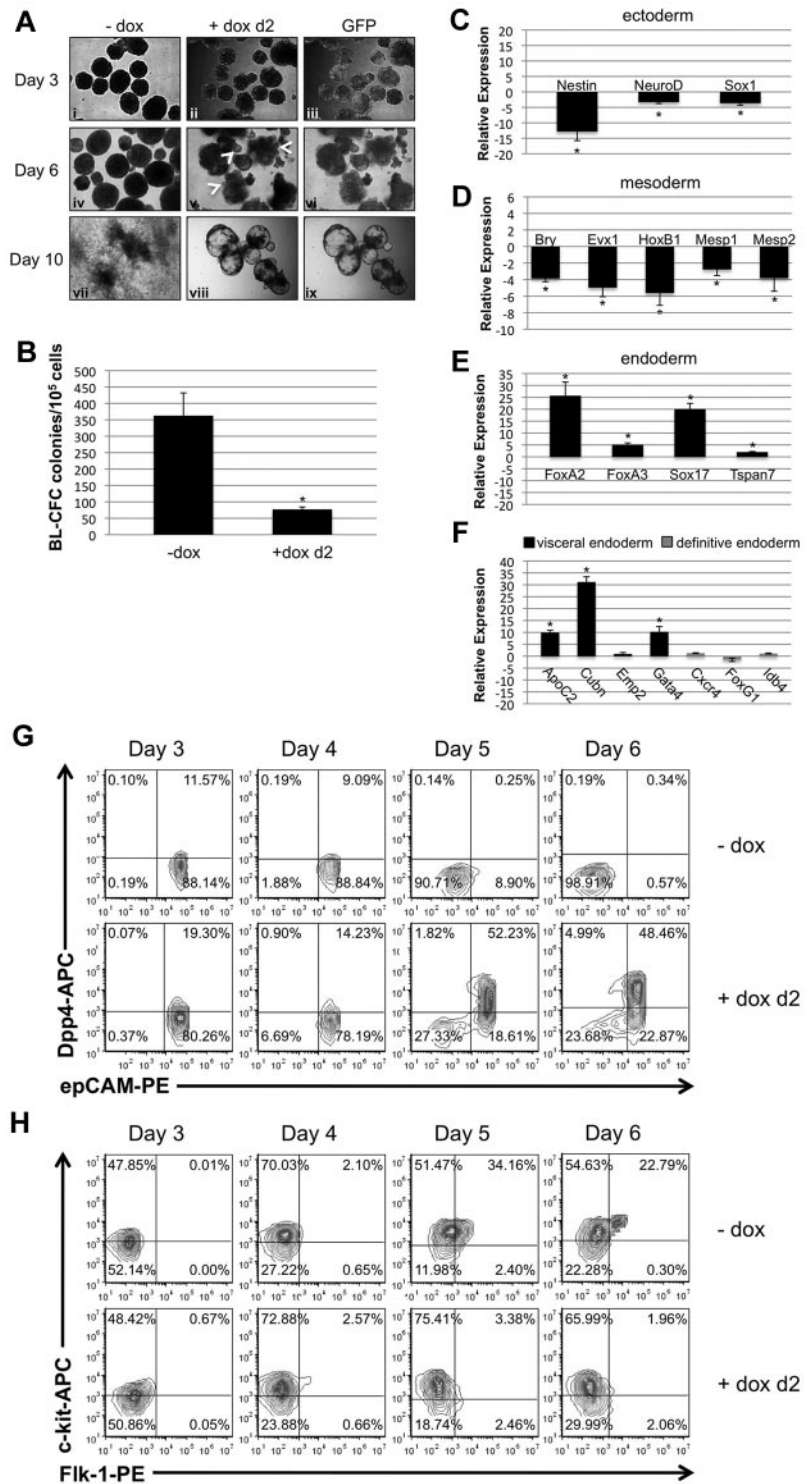
(Figure 2A). Conversely, when *Smad1* was depleted beginning on EB day 4, subsequent to progenitor commitment, there was an approximately 5-fold increase in the number of EryP colonies compared with uninduced controls (Figure 2A). This biphasic control of primitive hematopoiesis by *Smad1* is consistent with our previous published results,¹⁹ which suggested that *Smad1* expression after the early limited pulse abrogates progenitor expansion. To rule out potential confounding effects of doxycycline on cellular differentiation, *Smad1* knockdown was again induced on day 2 or 4 of EB differentiation, and doxycycline was also added directly to the erythroid-permissive methylcellulose differentiation medium. As shown in Figure 2B, the early suppression and late expansion of EryP potential was equivalent in terms of relative differences compared with uninduced controls, although the total number of EryP colonies was modestly reduced. These results demonstrate temporally separable and opposite functions for *Smad1* in primitive erythropoiesis.

Early depletion of *Smad1* impairs hematopoietic potential by affecting commitment of epiblast to derivatives

To investigate whether the phenotypes caused by early or late depletion of *Smad1* during EB differentiation differ mechanistically, EB morphology and gene expression patterns were evaluated comparatively. Figure 3A shows a panel of mi*Smad1* EBs on successive days of differentiation, either uninduced or after induction on day 2. Day 2–induced EBs expressed GFP throughout EB differentiation, initially ubiquitously but less so at later time points. The uninduced EBs displayed a characteristic round morphology with darker regions toward the center, indicative of developing mesoderm and its derivatives. In contrast, day 2–induced EBs formed vesiculated protrusions by day 4, which continued to emerge at the EB periphery through day 6 (see arrowheads Figure 3Av), by which time the EBs had become entirely cystic. Unlike control EBs, when these induced EBs were replated onto gelatinized dishes at day 7, they failed to adhere and flatten on the plate surface by day 10, as indicated in Figure 3Aviii and ix. Also unlike controls, they failed to exhibit any beating morphologies indicative of cardiac derivatives (data not shown). Because depletion of *Smad1* at day 2 of EB development ostensibly precedes commitment of epiblast to mesoderm and its derivative hemato-vascular progenitors,²⁶ we analyzed the hemangioblast analog BL-CFC colony-forming potential of day 2–induced EBs. As shown in Figure 3B, there was an approximately 5-fold reduction in BL-CFC potential, roughly equivalent to that observed for EryP potential (see Figure 2A).

Figure 3. Early depletion of *Smad1* results in disruption of epiblast derivatives and commitment to visceral endoderm.

(A) *Smad1* knockdown was induced on day 2 of EB differentiation, and EBs were analyzed for morphologic changes and GFP expression over the following several days. Induction was maintained by addition of doxycycline at day 5; day 7 EBs were transferred to gelatinized tissue-culture plates and examined both for their morphology and their ability to adhere to the plate surface. (B) Day 2–induced EBs were harvested at day 3.75 of differentiation and cultured in methylcellulose medium with cytokines permissive for differentiation into BL-CFC colonies. Colonies were identified and counted by their distinctive morphology 4 days later. For each sample, $n = 3$ and the graph is a representative example taken from a pool of at least 4 experiments. Error bars indicate SEM; $*P < .01$ compared with uninduced controls. Transcription of genes associated with ectoderm (C), mesoderm (D), endoderm (E), and, more selectively, visceral (F) and definitive endoderm (F) were analyzed by qPCR in day 4.5 EBs that had been induced at day 2. Data were analyzed using the $2^{-\Delta\Delta CT}$ method¹⁹ and reported as fold change in mRNA transcript level, and were normalized to control cells that were not treated with doxycycline. *Gapdh* transcript levels were used as a reference control, and shown are representative results from an experiment that was repeated at least 3 times. Error bars indicate SEM; $*P < .01$ compared with uninduced controls. (G) Visceral endoderm commitment in day 2–induced EBs was corroborated by flow cytometric analysis after staining for epCAM (pan-endoderm) and DPP4 (visceral endoderm)–specific fluorophore-conjugated Abs using cells from dissociated EBs over a 4-day time course from day 3 to day 6 of EB cultures. (H) FLK1 and c-KIT staining was analyzed from day 3 to day 6 by flow cytometry to measure the potential population of hematovascular precursors in EBs induced at day 2, compared with control uninduced samples.



These observations prompted us to investigate possible effects on germ layer development in *Smad1*-depleted EBs. Therefore, the expression of representative molecular markers was evaluated by quantitative real-time PCR (qPCR). For this purpose, EBs were induced for *Smad1* knockdown at day 2, and RNA was harvested at day 4.5 of EB differentiation. Compared with uninduced EBs, there was a statistically significant decrease in expression levels for ectoderm markers *Nestin*, *NeuroD*, and *Sox1* (Figure 3C), and mesoderm markers including *Brachyury*, *Evx1*, *HoxB1*, *Mesp1*, and *Mesp2* (Figure 3D). In contrast, there was a marked increase in the

expression levels for markers of endoderm generally (Figure 3E), and visceral endoderm specifically (Figure 3F). The pan-endodermal markers were all transcriptionally up-regulated compared with untreated controls, including *FoxA2* (≥ 20 -fold), *FoxA3* (≥ 5 -fold), *Sox17* (> 15 -fold), and *Tspan7* (> 3 -fold). While many genes are coexpressed in both primitive and definitive endoderm, several markers have been shown to discriminate endoderm types²⁷⁻²⁹ and we found that expression levels were enhanced particularly for genes associated with visceral endoderm. Transcript levels for apolipoprotein C2 (*ApoC2*; > 8 -fold), Cubilin

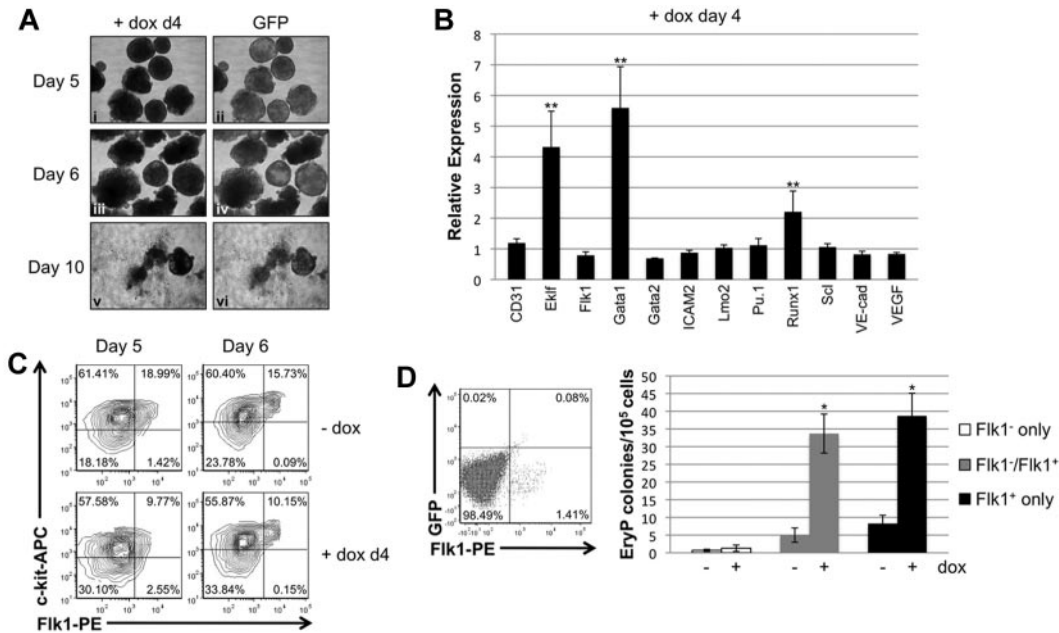


Figure 4. Late depletion of *Smad1* enhances erythroid potential correlating with enhanced expression levels for *Gata1*. (A) EBs induced on day 4 of differentiation examined for morphologic changes and GFP expression until day 6. EBs were transferred on day 7 to gelatinized tissue-culture plates and analyzed for their ability to adhere to the plate surface. (B) Hemangioblast marker gene expression was analyzed by qPCR; RNA from day 4–induced EBs was harvested after 24 hours, on day 5 of differentiation. Data were collected and analyzed using *Gapdh* as a reference control as in Figure 3B–E. Each experimental condition was repeated a minimum of 3 times and a representative result is shown. Error bars denote the SEM; ** $P < .01$ compared with uninduced controls. (C) Flow cytometric analysis of FLK1/c-KIT expression at days 5 or 6 of EB differentiation, after induction of *Smad1* depletion at day 4. (D) EryP colony-forming analysis of FLK1⁺ mesoderm sorted by flow cytometry from day 3.75 EBs to examine cell autonomy of *Smad1* functions. Defined populations were recultured as EBs for a further 2 days with or without day 4 doxycycline treatment, and disaggregated to generate primitive erythroid colonies under the relevant permissive conditions. Each experimental condition was repeated 3 times, and a representative result is shown. Error bars denote SEM; * $P < .05$ compared with uninduced controls.

(*Cubn*; > 25-fold), and *Gata4* (7-fold) were all considerably increased, while transcripts associated with definitive endoderm development, including *Cxcr4*, *Idb4*, and *FoxG1*, were not changed significantly (Figure 3F). Flow cytometry was used to analyze quantitatively cells that express epithelial cell adhesion molecule (epCAM) and dipeptidyl peptidase IV (DPP4), pan-endoderm and visceral endoderm markers, respectively.²⁷ As shown in Figure 3G, uninduced control EBs were depleted of epCAM⁺ cells by days 5–6 in culture. In contrast, *Smad1*-depleted EBs retained an epCAM⁺ population, a significant number (~50%) of which were epCAM⁺/DPP4⁺ double-positive cells.

Flow cytometry was also used to compare hemato-vascular development in control or day 2-induced EBs, by quantifying the emergence of FLK1⁺/c-KIT⁺ double-positive progenitors. In uninduced mi*Smad1* control EBs, FLK1⁺ cells began to accumulate on day 4 of differentiation, and by day 5, there was a significant population of clearly defined FLK1⁺/c-KIT⁺ double-positive cells (Figure 3H). In contrast, EBs induced for *Smad1* knockdown on day 2 exhibited severely diminished numbers of FLK1⁺ cells (~6% on day 5, Figure 3H), and a striking absence of double-positive cells even by day 6 (~2%). Overall, the data show that *Smad1* is essential from day 2 of EB differentiation for the commitment of epiblast to all 3 embryonic germ layers, and that *Smad1* depletion results in formation of predominantly visceral-like endoderm at their expense.

Depletion of *Smad1* after progenitor commitment increases hematopoietic potential through up-regulation of specific regulatory factors, including *Gata1*

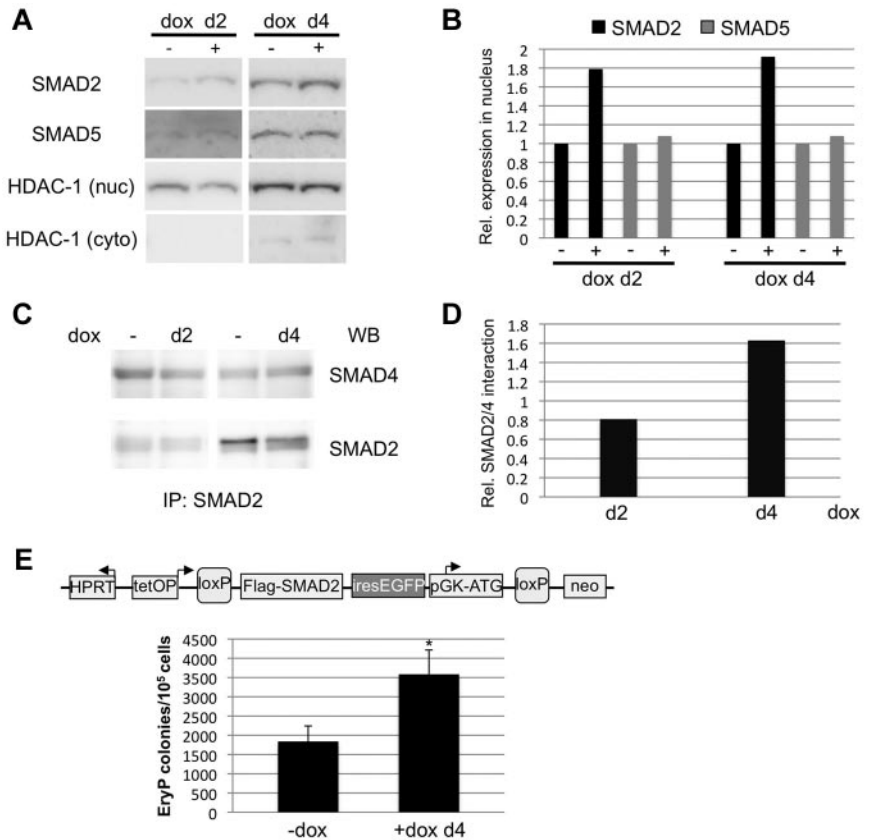
EB morphology and changes in gene expression were next evaluated after induction of *Smad1* knockdown starting at day 4 of

EB differentiation, at a time subsequent to specification of the hemato-vascular lineage. When induced on day 4 of differentiation, EBs were generated that on subsequent days were qualitatively similar to uninduced control EBs (Figure 4A). Moreover, day 4-induced EBs that were replated on gelatinized plates at day 7 generally adhered to the surface, although with some morphologic heterogeneity compared with control samples.

To investigate changes in the transcriptional program in response to late depletion of *Smad1*, the expression levels of transcripts associated with the hemangioblast or hematopoietic progenitors were evaluated by qPCR. When *Smad1* knockdown was induced at day 4 there was already by day 5 more than a 5-fold increase in transcript levels for *Gata1* (Figure 4B). In addition, transcript levels for the hematopoietic genes *Eklf* and *Runx1* were significantly increased compared with uninduced controls. In contrast, transcript levels for hemangioblast-associated genes, including *Flk1*, *Gata2*, *Lmo2*, *Scl*, and *Vegf*, were unaffected or slightly decreased (Figure 4B). These results suggest that inhibitory effects of *Smad1* on hematopoietic potential function at least in part through restricting levels of transcriptional activators including *Gata1*, and are consistent with an effect on committed hematopoietic progenitors rather than earlier mesoderm or hemangioblast cells. When depletion was induced at day 4, *Flk1* expression levels persisted through days 5–6, as did the FLK1⁺/c-KIT⁺ double-positive population (Figure 4C). To probe whether *Smad1* function is cell autonomous for hematopoietic progenitors, the initial wave of FLK1⁺ cells was isolated from day 4 EBs by cell sorting, and then recultured separately or after recombination with FLK1⁻ cells, under conditions of doxycycline-induced *Smad1* depletion, and analyzed for erythroid progenitor potential. As shown in Figure 4D, induction of *Smad1* knockdown specifically in this initial wave of

Figure 5. Smad1 knockdown correlates with activation of SMAD2, a TGF- β downstream effector.

(A) miSmad1 EBs were left untreated or induced with 1 μ g/mL doxycycline to deplete *Smad1* on day 2 or day 4, and EBs were harvested and fractionated to generate nuclear extracts. Nuclear fractions were subjected to Western blotting to quantify SMAD2 and SMAD5 levels, and HDAC-1 was used as a loading control for total nuclear protein. (B) Densitometric analysis of relative nuclear SMAD2 and SMAD5 protein levels, with induced samples normalized to uninduced controls. (C) Whole-cell lysates were generated from day 2- or day 4-induced miSmad1 EBs and subjected to immunoprecipitation using a SMAD2-specific Ab. Immunoprecipitates were analyzed by Western blotting for SMAD2 and SMAD4. (D) Densitometric quantification of SMAD2/SMAD4 interaction, with day 2- and day 4-induced samples normalized to their respective uninduced controls. (E) An ES-cell line was engineered to allow doxycycline-induced expression of *Smad2* (see supplemental Figure 1). *Smad2* expression was induced on day 4 and on day 5.75 the EBs were analyzed for EryP colony-forming potential, as in Figure 2. For each sample, n = 3, and the graph is a representative example taken from a pool of at least 4 experiments. Error bars indicate SEM; **P* < .01 compared with uninduced controls.



FLK1⁺ hemato-vascular precursors is fully sufficient to expand erythroid progenitors, consistent with a cell-autonomous function for *Smad1*, or at least function within the FLK1⁺ progenitor population.

SMAD2 provides a mechanistic link between the BMP and TGF- β pathways in the context of *Smad1* knockdown

BMP-responsive SMADs and TGF- β -responsive SMADs all function via the common co-SMAD, SMAD4. Therefore, it is possible for SMADs to compete for activity with each other, if SMAD4 levels are limiting. In the context of the EBs derived from miSmad1ES cells, depletion of *Smad1* could result indirectly in enhanced activity of *Smad5*, or even of *Smad2/3*, the latter of which would imply a shift to a predominantly TGF- β -like activated pathway. To evaluate this possibility, the relative levels of nuclear SMAD2/3 (Abs do not distinguish) and SMAD5 were measured after depletion of *Smad1* for 24 hpf. As shown in Figure 5A and B, levels of nuclear SMAD2 increased approximately 2-fold, while nuclear SMAD5 levels remained unchanged. Although nuclear SMAD2 increased on either day 2 or day 4 induction of *Smad1* knockdown, SMAD2/SMAD4 complexes increased only with day 4 induction, which is the timing relevant to the observed hematopoietic increase (Figure 5C-D). To test directly if *Smad2/3* activity can enhance hematopoietic fate, in the absence of *Smad1* depletion, we generated a new ES-cell line, with *Smad2* placed under doxycycline control (iSmad2ES cells, supplemental Figure 1). In EBs derived from these iSmad2ES cells, induction of SMAD2 expression on day 4 resulted in an approximately 2-fold expansion of EryP colonies (Figure 5E). These results are consistent with the hypothesis that depletion of *Smad1* leads to enhanced SMAD2 activity, which impacts hematopoietic progenitor fate.

Knockdown of *Smad1* after hematopoietic commitment expands progenitors for other lineages, including definitive erythroid and multipotent progenitors

Finally, the ability of *Smad1* levels to regulate the development of other hematopoietic progenitors was tested. The potential of day 2- and day 4-induced EBs to form colonies was quantitatively evaluated for progenitors to macrophages (MacP) and megakaryocytes (MegaP), as well as to definitive erythroid (EryD) and multilineage mixed colonies consisting of macrophages, megakaryocytes, erythroid cells, and granulocytes. Hematopoietic colonies were identified and scored using the morphologic criteria established by Kennedy and Keller.²¹ As expected, based on the effects on mesoderm development, induction of *Smad1* knockdown on day 2 of EB development led to a consistent reduction in formation of all hematopoietic colonies compared with uninduced controls (Figure 6). Conversely, when EBs were induced at day 4, there was an increase in progenitor colony potential compared with uninduced controls (Figure 6A-B), regardless of the lineage. When *Smad1* was depleted starting at day 4, the potential for MacP, MegaP, and EryD colony generation was enhanced approximately 5-fold, while the numbers of mixed lineage colonies showed a slightly more modest increase of approximately 3-fold (Figure 6).

Discussion

We developed a conditional shRNA-mediated knockdown system in ES cells to study the role of *Smad1* in hematopoietic development throughout EB differentiation. The system allows us to study in vitro the function of a gene knockdown that is otherwise early embryonic lethal. It also provides an advantage compared with

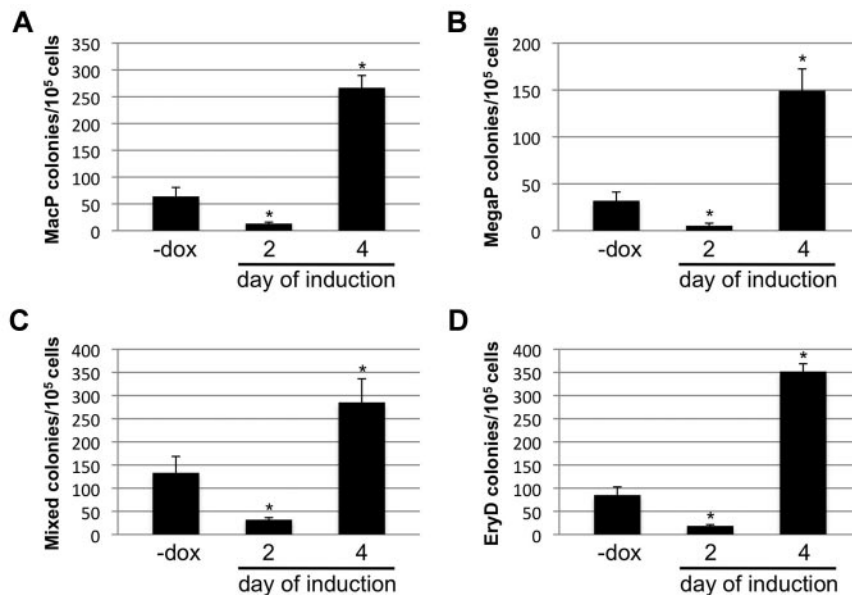


Figure 6. The biphasic effects of *Smad1* on EB-derived EryP potential extend to other hematopoietic progenitors. The miSmad1 EBs were left untreated or induced with doxycycline on day 2 or day 4, and day 5.75 EBs were harvested and recultured in semisolid methylcellulose media permissive for differentiation into (A) macrophage (MacP) colonies, (B) megakaryocyte (MegaP) colonies, (C) definitive mixed lineage colonies, or (D) EryD definitive erythroid colonies. After replating dissociated EBs in media containing the relevant permissive cytokines, MacP, MegaP, and EryD colonies were identified by their distinctive morphologies and counted on day 7; mixed lineage colonies were counted on day 9. For each sample, $n = 3$, and each graph is a representative example taken from a pool of at least 4 experiments. Error bars indicate SEM; * $P < .01$ compared with uninduced controls.

using extracellular inhibitors of BMP signaling, such as NOGGIN, because considerable regulatory potential may be revealed by distinct pathway-restricted SMAD genes. Previously we used a complementary ES-cell line for temporally controlled *Smad1* expression. While *Smad1* was sufficient to promote hemangioblast and hematopoietic fate, this only occurred if the induction was transient; unless induction of *Smad1* expression was arrested, the expansion failed to occur. This intriguing result led us to hypothesize that prehematopoietic mesoderm is receptive to *Smad1*-mediated expansion, while the pool of committed progenitors is, in contrast, restricted by *Smad1*. In the present study, we provide direct evidence for this hypothesis. Knockdown of *Smad1* on day 2, before hemangioblast commitment,⁶ severely limits the potential for hematopoiesis; this phenotype is the opposite of that seen for *Smad1* forced expression. This deficit is likely because of a limited pool of epiblast-derived mesoderm precursors, as shown by the decreased levels of transcripts for ectoderm and mesoderm markers. There is instead a marked shift in these EBs toward primitive endoderm character. The mouse *Smad1* knockout shows defects in extra-embryonic development, including overgrowth of the posterior visceral endoderm.¹⁵ Thus, at least some aspects of the mouse mutant appear to be recapitulated in the miSmad1ES-cell model. The gain in primitive endoderm at the expense of mesoderm could be caused in part by deregulated cross-talk between BMP and TGF- β signaling pathways. We found in Western blotting experiments that depletion of SMAD1 leads to a corresponding increase in the levels of nuclear SMAD2. It is well established that *Smad2*-dependent *Nodal/ActivinA* signaling promotes endoderm fate in EB cultures,³⁰ although this promotes definitive endoderm rather than the primitive endoderm type that predominates in the *Smad1* knockdown cultures. Interestingly, we found a very similar phenotype, with directed differentiation of CXCR4-negative, DPP4⁺ primitive endoderm, when *Gata4* is expressed in EBs, starting at day 2.²⁸ *Gata4* levels are enhanced in the *Smad1* knockdown cultures. Therefore, *Smad1* might function by restricting the *Gata4*-dependent derivation of primitive endoderm, allowing normal germ layer specification to proceed.

In contrast, induction of *Smad1* knockdown after germ layer specification and hemangioblast commitment, but before hematopoietic differentiation, results in an expansion of hematopoietic potential. Notably, the level of this expansion (5-fold) is equivalent

to the level that expansion is blocked by continuous forced expression of *Smad1* during this same developmental period (5-fold). This effect is unrelated to development of hematopoietic mesoderm or the hemangioblast. First, the timing of the effect is consistent with expansion of already committed progenitors, and is cell-autonomous, because *Smad1* depletion in FLK1⁺ precursors is sufficient to cause the observed relative increase in hematopoietic progenitors. Second, it correlates with a significant increase in expression levels of hematopoietic-specific genes *Gata1*, *Eklf*, and *Runx1*, but not other regulatory genes including *Scl* and *Lmo2* that are more associated with the earlier hemato-vascular progenitors. Because activation of *Gata1* is necessary for erythroid survival and differentiation, and it has been reported that SMAD5 specifically up-regulates expression of both *Gata1* and *Eklf*^{31,32}, we tested whether the depletion of *Smad1* causes enhanced activation of *Smad5*. However, in contrast to SMAD2, levels of nuclear SMAD5 are unchanged by *Smad1* depletion. In any event, the discrepancy between expression of *Gata1* and *Runx1* versus *Scl* and *Lmo2* suggests an uncoupling of the transcriptional network responsible for the initial commitment of the hemato-vascular lineage.

We report an approximately 50% reduction of SMAD1 in cultured EBs, but this is not comparable with a heterozygous mutant ESC line or mouse, because quantification is a sum average of the population of cells at one snap-shot timepoint. The knockdown will vary in different cells at different timepoints, and we likely reduce SMAD1 below a functional threshold in some (but perhaps not all) progenitors during the course of our knockdown experiments. In this context, the results we present may underestimate the function for SMAD1 because with a greater knockdown, the changes in developmental potential might be even more dramatic.

Although we focused on erythroid regulatory genes, progenitors for other lineages, including myeloid cells are similarly enhanced. Our limited analysis showed increased levels of some relevant regulatory genes (*Runx1*), but not others (such as *Pu.1*). This might simply be because of relatively low levels of myeloid progenitors in the EB cultures (increasing the noise to signal ratio in whole EB samples) or to differences in timing for when the progenitors expand. Our studies suggest that cross-talk between BMP and TGF- β -like signaling components may influence embryonic hematopoiesis. This could occur, as we suggest, by relatively direct

signaling component cross-talk, or *Smad2* activity could be enhanced indirectly by *Smad1* depletion. It may be interesting to explore whether this has clinical relevance for BM hematopoiesis, given that constitutive activation of *Smad2* is associated with ineffective hematopoiesis in myelodysplastic syndrome.³³

Acknowledgments

We thank Ting-Chun Liu for her valuable technical contributions.

This work was supported by National Institutes of Health (NIH) grant R37HL056182 (T.E.). B.D.C. is supported by NIH training grant T32HL083824.

References

- McGrath KE, Palis J. Hematopoiesis in the yolk sac: more than meets the eye. *Exp Hematol*. 2005;33(9):1021-1028.
- Lacaud G, Keller G, Kouskoff V. Tracking mesoderm formation and specification to the hemangioblast in vitro. *Trends Cardiovasc Med*. 2004;14(8):314-317.
- Soderberg SS, Karlsson G, Karlsson S. Complex and context dependent regulation of hematopoiesis by TGF-beta superfamily signaling. *Ann N Y Acad Sci*. 2009;1176:55-69.
- Winnier G, Blessing M, Labosky PA, Hogan BL. Bone morphogenetic protein-4 is required for mesoderm formation and patterning in the mouse. *Genes Dev*. 1995;9(17):2105-2116.
- Kishigami S, Mishina Y. BMP signaling and early embryonic patterning. *Cytokine Growth Factor Rev*. 2005;16(3):265-278.
- Choi K, Kennedy M, Kazarov A, Papadimitriou JC, Keller G. A common precursor for hematopoietic and endothelial cells. *Development*. 1998;125(4):725-732.
- Johansson BM, Wiles MV. Evidence for involvement of activin A and bone morphogenetic protein 4 in mammalian mesoderm and hematopoietic development. *Mol Cell Biol*. 1995;15(1):141-151.
- Beppu H, Kawabata M, Hamamoto T, et al. BMP type II receptor is required for gastrulation and early development of mouse embryos. *Dev Biol*. 2000;221(1):249-258.
- Moustakas A, Heldin CH. The regulation of TGF-beta signal transduction. *Development*. 2009;136(22):3699-3714.
- Arnold SJ, Maretto S, Islam A, Bikoff EK, Robertson EJ. Dose-dependent *Smad1*, *Smad5* and *Smad8* signaling in the early mouse embryo. *Dev Biol*. 2006;296(1):104-118.
- Larsson J, Karlsson S. The role of *Smad* signaling in hematopoiesis. *Oncogene*. 2005;24(37):5676-5692.
- Chang H, Huylebroeck D, Verschuere K, Guo Q, Matzuk MM, Zwijsen A. *Smad5* knockout mice die at mid-gestation due to multiple embryonic and extraembryonic defects. *Development*. 1999;126(8):1631-1642.
- Yang X, Castilla LH, Xu X, et al. Angiogenesis defects and mesenchymal apoptosis in mice lacking *SMAD5*. *Development*. 1999;126(8):1571-1580.
- Lechleider RJ, Ryan JL, Garrett L, et al. Targeted mutagenesis of *Smad1* reveals an essential role in chorioallantoic fusion. *Dev Biol*. 2001;240(1):157-167.
- Tremblay KD, Dunn NR, Robertson EJ. Mouse embryos lacking *Smad1* signals display defects in extra-embryonic tissues and germ cell formation. *Development*. 2001;128(18):3609-3621.
- Dick A, Meier A, Hammerschmidt M. *Smad1* and *Smad5* have distinct roles during dorsoventral patterning of the zebrafish embryo. *Dev Dyn*. 1999;216(3):285-298.
- McReynolds LJ, Gupta S, Figueroa ME, Mullins MC, Evans T. *Smad1* and *Smad5* differentially regulate embryonic hematopoiesis. *Blood*. 2007;110(12):3881-3890.
- Murry CE, Keller G. Differentiation of embryonic stem cells to clinically relevant populations: lessons from embryonic development. *Cell*. 2008;132(4):661-680.
- Zafonte BT, Liu S, Lynch-Kattman M, et al. *Smad1* expands the hemangioblast population within a limited developmental window. *Blood*. 2007;109(2):516-523.
- Sun D, Melegari M, Sridhar S, Rogler CE, Zhu L. Multi-miRNA hairpin method that improves gene knockdown efficiency and provides linked multi-gene knockdown. *Biotechniques*. 2006;41(1):59-63.
- Kennedy M, Keller GM. Hematopoietic commitment of ES cells in culture. *Methods Enzymol*. 2003;365:39-59.
- Livak KJ, Schmittgen TD. Analysis of relative gene expression data using real-time quantitative PCR and the 2(-Delta Delta C(T)) method. *Methods*. 2001;25(4):402-408.
- Andrews NC, Faller DV. A rapid micropreparation technique for extraction of DNA-binding proteins from limiting numbers of mammalian cells. *Nucleic Acids Res*. 1991;19(9):2499.
- Kyba M, Perlingeiro RC, Daley GQ. *HoxB4* confers definitive lymphoid-myeloid engraftment potential on embryonic stem cell and yolk sac hematopoietic progenitors. *Cell*. 2002;109(1):29-37.
- Keller GM. In vitro differentiation of embryonic stem cells. *Curr Opin Cell Biol*. 1995;7(6):862-869.
- Kattman SJ, Adler ED, Keller GM. Specification of multipotential cardiovascular progenitor cells during embryonic stem cell differentiation and embryonic development. *Trends Cardiovasc Med*. 2007;17(7):240-246.
- Sherwood RI, Jitiani C, Cleaver O, et al. Prospective isolation and global gene expression analysis of definitive and visceral endoderm. *Dev Biol*. 2007;304(2):541-555.
- Holtzinger A, Rosenfeld GE, Evans T. *Gata4* directs development of cardiac-inducing endoderm from ES cells. *Dev Biol*. 2007;317(1):63-73.
- Hou J, Charters AM, Lee SC, et al. A systematic screen for genes expressed in definitive endoderm by serial analysis of gene expression (SAGE). *BMC Dev Biol*. 2007;7:92.
- Kubo A, Shinozaki K, Shannon JM, et al. Development of definitive endoderm from embryonic stem cells in culture. *Development*. 2004;131(7):1651-1662.
- Adelman CA, Chattopadhyay S, Bieker JJ. The BMP/BMPR/*Smad* pathway directs expression of the erythroid-specific *EKLF* and *GATA1* transcription factors during embryoid body differentiation in serum-free media. *Development*. 2002;129(2):539-549.
- Lohmann F, Bieker JJ. Activation of *Eklf* expression during hematopoiesis by *Gata2* and *Smad5* prior to erythroid commitment. *Development*. 2008;135(12):2071-2082.
- Zhou L, Nguyen AN, Sohal D, et al. Inhibition of the TGF-beta receptor I kinase promotes hematopoiesis in MDS. *Blood*. 2008;112(8):3434-3443.

Authorship

Contribution: B.D.C. conceived the study, carried out the experiments, and wrote the manuscript; S.L. carried out experiments and provided technical expertise; and T.E. conceived the study and wrote the manuscript.

Conflict-of-interest disclosure: The authors declare no competing financial interests.

Correspondence: Todd Evans, Department of Surgery, Weill Cornell Medical College, 1300 York Ave, LC-709, New York, NY 10065; e-mail: tre2003@med.cornell.edu.